Reaction Field (RF) Calculation of the Spectral Shifts of Indole

C. F. Chabalowski
U.S. ARMY RESEARCH LABORATORY

D. R. Garmer
MT. SINAI MEDICAL CENTER

J. O. Jensen
U.S. ARMY EDGEWOOD RESEARCH, DEVELOPMENT, AND ENGINEERING CENTER

M. Krauss
NATIONAL INSTITUTE OF STANDARDS AND TECHNOLOGY

ARL-TR-677   January 1995

19950131 057

DTIC
SELECTED
FEB, 0 7 1995
B

NOTICES

REPORT DOCUMENTATION PAGE

1. AGENCY USE ONLY (Leave blank)	2. REPORT DATE January 1995	3. REPORT TYPE AND DATES COVERED Final, Sep 91–Mar 93

4. TITLE AND SUBTITLE

Reaction Field (RF) Calculation of the Spectral Shifts of Indole

5. FUNDING NUMBERS

PR: 1L161102AH43

6. AUTHOR(S)

C. F. Chabalowski, D. R. Garmer,* J. O. Jensen,** and M. Krauss***

7. PERFORMING ORGANIZATION NAME(S) AND ADDRESS(ES)

U.S. Army Research Laboratory
ATTN: AMSRL-WT-PC
Aberdeen Proving Ground, MD 21005-5066

8. PERFORMING ORGANIZATION REPORT NUMBER

9. SPONSORING/MONITORING AGENCY NAME(S) AND ADDRESS(ES)

U.S. Army Research Laboratory
ATTN: AMSRL-OP-AP-L
Aberdeen Proving Ground, MD 21005-5066

10. SPONSORING/MONITORING AGENCY REPORT NUMBER

ARL-TR-677

11. SUPPLEMENTARY NOTES
*Department of Physiology and Biophysics, Mt. Sinai Medical Center, New York, NY 10029; **U.S. Army Chemical Research, Development, and Engineering Center, Aberdeen Proving Ground, MD 21010; ***Center of Advanced Research in Biotechnology, National Institute of Standards and Technology, Gaithersburg, MD 20899

12a. DISTRIBUTION/AVAILABILITY STATEMENT
Approved for public release; distribution is unlimited.

12b. DISTRIBUTION CODE

13. ABSTRACT (Maximum 200 words)

The excitation energy of indole has been investigated at geometries relevant to both the absorption and emission spectra using first-order configuration interaction (FOCI) methods. The calculation focused on the shift in the relative energy between the two excited states, L_B and L_A, and the excitation energies with geometry. A reaction field (RF) calculation also examined the shift in excitation energies when the molecule is dissolved in water. The excited states are found to be separated in vacuo by about 4,500 cm^{-1} at both the ground state and an approximation to the equilibrium L_B geometry, M, and by 2,500 cm^{-1} at the optimized geometry of both the first triplet excited state, T, and the first excited singlet state represented by a singles-only configuration interaction (S1). In water, the excited states are essentially degenerate and mixed at the ground-state geometry. However, at the excited-states geometries, M and T, the L_A state is shifted lower in energy than the L_B state due to the large L_A excited-state RF. At the S1 geometry, the electronic behavior of the two excited states is different from that at the other geometries. An approximation to the L_A state is now the lower state both in vacuo and in the presence of the RF. There is a large calculated solvent fluorescent red shift in water at any geometry as well as a substantial Franck-Condon (FC) shift due to the steeper energy surface in the ground state compared to the excited states. The calculated energy shifts, dipole moments, and relative transition dipoles are in qualitative accord with experiment. However, the calculated fluorescent reaction dipoles are substantially larger than estimated in earlier studies.

14. SUBJECT TERMS

spectroscopy of indole, solvent effect, reaction field theory

15. NUMBER OF PAGES
22

16. PRICE CODE

17. SECURITY CLASSIFICATION OF REPORT	18. SECURITY CLASSIFICATION OF THIS PAGE	19. SECURITY CLASSIFICATION OF ABSTRACT	20. LIMITATION OF ABSTRACT
UNCLASSIFIED	UNCLASSIFIED	UNCLASSIFIED	SAR

INTENTIONALLY LEFT BLANK.

TABLE OF CONTENTS

INTENTIONALLY LEFT BLANK.

LIST OF FIGURES

LIST OF TABLES

INTENTIONALLY LEFT BLANK.

1. INTRODUCTION

Indole is the simplest model for studying the spectroscopy of tryptophan-containing proteins. Considerable interest has focused on the large fluorescent red shift in polar solvents (Creed 1984), but the electronic structure and relative energetics of the two singlet excited states (designated L_B and L_A for the first and second states, respectively) in vacuo must be understood for a theoretical analysis of the solvent perturbations. The first and second excited states in absorption are designated L_B and L_A for historical reasons. These designations are maintained for calculations at the ground-state geometry, and the similarity of the electronic behavior at other geometries is used to follow and characterize the states. A thorough semiempirical analysis of the electronic structure of indole and the excited states has been developed (Callis 1991). Such calculations assist in the assignment of absorption origins of the two excited states for the spectra in the gas phase or water (Ilich, Haydock, and Prendergast 1989) and for various indoles dissolved in either cyclohexane or butanol (Anderson et al. 1986; Rehms and Callis 1987). However, in the analysis of near-ultraviolet (UV) fluorescent excitation spectra there has been no success in explicitly identifying the second excited state (Bersohn, Even, and Jortner 1984; Hager and Wallace 1984; Rizzo, Park, and Levy 1986). It has been suggested that, in the gas phase, the N–H bond may dissociate in this state and not fluoresce (Glasser and Lami 1981; Lami and Glasser 1986; Hager, Demmer, and Wallace 1987; Demmer et al. 1990). Mixing of the two excited states also was shown to depend on the proton donation of the solvent molecule to the π density of the indole (Tubergen and Levy 1991). Energy surface and electronic characteristics of the excited states in vacuo and in the presence of solvent are then important to understanding both the absorption and fluorescent Franck–Condon (FC) envelopes. The semiempirical calculations cannot vary the geometry without introducing more parameters. Semiempirical studies must choose from a wide parameter space, and this is difficult even when the experimental situation has the utmost clarity, which is not true for indole. An ab initio study is then warranted even at the ground-state geometry, and fluorescence properties require calculations at an approximation to the excited-state geometries.

A number of different models have been presented for the fluorescent red shift (Creed 1984), but we will explore only the one assuming solvent reorganization in the excited state (Lami and Glasser 1986; Hager, Demmer, and Wallace 1987; Demmer et al. 1990; Tubergen and Levy 1991; Suppan 1990). The influence of the media on the spectroscopic transitions is estimated from the solute dipole-solvent reaction dipole interaction. Dipole moments of the electronic states are obtained by ab initio quantum calculations and the solvent effect obtained by both classical (Suppan 1990) and quantum methods (Karelson and

1

Zerner 1990; Wong, Frisch, and Wiberg 1991; Karelson and Zerner 1992; Garmer 1992; Krauss and Garmer 1993). Although reaction field (RF) models within the semiempirical theories are well established (Karelson and Zerner 1990; 1992), again it is difficult to obtain the electronic and energetic changes that occur with the combined effects of geometry and solvent perturbations. An ab initio description can provide insight into the electronic structure of the excited states and, therefore, into the unusual fluorescent red shift observed for indole.

The adiabatic dissociation behavior of the ground and excited states will also be analyzed. In a previous study (Krauss and Garmer 1993), we have calculated the excited-state spectrum of the neutral indole radical produced by dissociating the N–H bond. From this catalog of excited states, we know the order of the σ and π radicals and can deduce the possibility of barriers as well as determine which excited states are above dissociation limits.

2. METHOD

The electronic description of the excited states requires a multiconfiguration representation. This is especially true when the RF perturbs and shifts these states. A balanced treatment of the correlation in the ground and excited states can be approached by means of first-order configuration interaction (FOCI) calculations (Krauss and Roszak 1992). The reference space for the FOCI provides all possible couplings among the chosen active orbitals. All configurations generated in this reference space interact through the all-electron Hamiltonian. Single excitations from this base set of configurations into the virtual space relaxes the originally chosen set of active or valence (V) orbitals. Interactions among the reference configurations and all configurations arising by single excitation from the reference set yield an FOCI secular equation which is solved for the relevant number of V states. The molecular orbital basis can then be improved by iterating with the natural orbitals obtained from the configuration interaction (CI) wave functions (Bender and Davidson 1966).

All FOCI calculations were done with the GAMESS system of codes (Schmidt et al. 1987) modified by inclusion of the dipole RF into the Hamiltonian (Garmer 1992; Krauss and Garmer 1993). The perturbation couples the molecular dipole and the RF, $H' = -\mu R_i$, with $R_i = \left(\mu_i / a^3\right) 2f(D)$, where $f(D) = (D-1)/(2D+1)$ and D is the dielectric constant. The total energy includes the solvent polarization. The reaction field, R, for the dipole-dipole interaction between the solute and solvent is

2

determined by the initial state dipole moment, μ_i, of the radiating system. Although the radius a has been related to the volume of the molecule, it is essentially an artifact of the multipolar expansion and may be smaller than the molecular radius. The water is presumed to relax and orient by the dipolar field of either the ground state in absorption or the excited state in fluorescence in an FC transition. The classical shift formula is given by Suppan (1990),

$$\Delta E_{ge} = -\mu_g \left(\mu_e - \mu_g\right) a^{-3} \left[2\left(f(D) - g(n)\right)\right] - \left(\mu_e^2 - \mu_g^2\right) a^{-3} g(n),$$

with $g(n) = \left(n^2 - 1\right)/\left(2n^2 + 1\right)$ and n being the refractive index. The classical expression assumes that the radiative transition is sufficiently fast that the water molecules do not relax during the transition but the solvent polarization responds to both the ground- and excited-state dipole moments. The dipole moments used in the classical shift formula are obtained with the RF FOCI. The quantum calculation as opposed to the classical analysis does not distinguish between coupling time scales and assumes that the perturbation, H', is present during the transition and acts on both initial and final states.

Since we are interested in both the absorption and fluorescent transitions, geometries were obtained by gradient optimizations for both the ground and excited states. Closed and open shell restricted Hartree–Fock SCF optimizations obtained ground (X) and triplet (T) excited-state geometries in single configuration calculations using a double-zeta level basis with K-shell orbitals replaced by compact effective core potentials (Stevens, Basch, and Krauss 1984). Gaussian 90 (Frisch et al. 1990) was used to obtain estimates of the geometry of the first excited singlet state in two ways. First, the excited-state geometry was optimized in a complete active space multiconfiguration self-consistent-field (CAS-MCSCF) calculation, where four electrons were distributed among four π orbitals using a 3/21G basis. This MCSCF optimization did converge for a first excited state (M), yielding a geometry substantially different from the triplet one. It is expected that the M geometry is closer to the equilibrium geometry of the L_B state since it is determined by optimizing the dominant π to π^* excitations. Second, the CI singles approach in Gaussian (Frisch et al. 1990; Foresman et al. 1992) was used to optimize the geometries for the lowest two excited singlets, and both excited states had bond distances that were different from either T or M. As opposed to the T and M structures where excitations are localized to the benzene ring, the C_2–C_3 bond on the pyrrole ring is also affected. The energies from the first excited-state structure, S1, are reported in Table 1 as an example of this family of structures because the C_2–C_3 bond is lengthened

3

Table 1. Total Energies (Hartree), Dipole Moments (e-bohr), and Excitation Energetics (cm^{-1})

A. In Vacuo Indole FOCI Energies (−E) and Dipole Moments

State		X	T	M	S1
1		57.57781	57.55630	57.56236	57.57094
		0.79	0.84	0.84	0.78
	exp[a]	0.84			
2		57.38487	57.38512	57.38995	57.37806
		0.83	0.88	0.85	1.37
	exp[b]	0.90			
3		57.36448	57.37498	57.36920	57.36725
		2.30	2.54	2.55	0.938
	exp[b]	2.12			

B. RF Indole FOCI Energies (−E) and Dipole Moments

State	X			
	RF-X		RF-L$_A$	
1	57.57931	57.57948	57.57736	57.57613
	1.06	1.16	1.59	1.74
2	57.38630	57.38650	57.38745	57.38739
	1.13	1.25	2.37	2.78
3	57.36942	57.37091	57.37672	57.37689
	2.57	2.65	2.69	2.59

State	RF-L$_A$					
	T		M		S1	
1	57.55544	57.55002	57.56138	57.55610	57.57194	57.56994
	1.75	2.18	1.73	2.13	1.21	1.52
2	57.39215	57.39535	57.38854	57.38913	57.38377	57.38598
	3.69	4.17	1.54	4.10	2.27	2.73
3	57.38400	57.37795	57.38614	57.38238	57.36796	57.36504
	1.61	1.97	3.66	1.86	1.06	1.26

[a]See Lami and Glasser (1986).
[b]Experimental data for excited states are summarized in Callis (1991).

Table 1. Total Energies (Hartree), Dipole Moments (e-bohr), and Excitation Energetics (cm^{-1})
(Continued)

C. Relative FOCI Energetics					
ΔE	X	T	M	S1	RF
12	42,347	37,571	37,836	42,332	none
	41,682	35,836	37,935	41,299	L_A, 1
	41,422	33,946	36,645	40,375	L_A, 2
	42,360				X, 1
	42,353				X, 2
	34,965				exp
13	46,820	39,797	42,390	44,705	none
	44,036	37,625	38,461	44,768	L_A, 1
	43,728	36,793	38,127	44,970	L_A, 2
	46,066				X, 1
	45,777				X, 2
	37,635				exp
23	4,473	2,226	4,554	2,373[a]	none
	2,354	−1,789	526	3,470[a]	L_A, 1
	2,306	−2,847	−1,482	4,596[a]	L_A, 2
	3,706				X, 1
	3,424				X, 2
ΔE	T-X		M-X	S1-X	RF
11′	4,721		3,392	1,507	none
33′	−2,303		−1,035	−608	none

[a]Assuming ΔE_{23} is equivalent to ΔE_{AB}, then these values are all negative.

in S1. This bond has been singled out as relevant to curve crossing between the two excited states (Callis 1991), and a comparison of energies at S1 with the other three is of interest. The structure optimized for the second excited state actually yielded substantially the highest energy for this state among all of the geometries at comparable FOCI calculations. The excited-states energy separation was also much larger than that at any other geometry and is not considered further. The internal coordinates for the four optimized structures are given in the supplementary material. There is no gas-phase indole structure, but the indole group has been determined in two crystal structures (Karle, Britts, and Gum 1964; Takigawa et al. 1966); these structures differ from each other as much as they do from the theoretical one. More accurate theoretical ground-state structures can easily be generated using direct Moller–Plesset methods, but the present structure is compatible with and at a comparable level of accuracy with the

excited states. The excited-state geometries all represent V structures with one π bond broken. Bond distances and a V schematic are given in Figure 1, where we see that T shows one specific bond structure but M and S1 are a mixture of resonance bond structures.

The excited-state calculations are found to require excitations from the tightly bound orbitals. Therefore, a minimum of 10 doubly (D) occupied orbitals is found necessary in the active space of the FOCI. This requirement limited the number of V orbitals in the active space to one, so the total number of configurations does not become unmanageable in GAMESS. In a previous study of the indole radicals, only one V orbital was needed (Krauss and Garmer 1993). The FOCI does provide for some of the contributions of such V orbitals through single excitations into the virtual space, and the natural orbital occupancy of the second V orbital is significant for one of the excited states. This limitation in the number of V orbitals undoubtedly limits the absolute accuracy of the excitation energies. The largest active space that was used for the data in Table 1 included 15 D orbitals. Increasing the number of D orbitals from 10 to 15 determined that the energy difference of the excited states as well as their excitation energy decreased slightly. The dissociation energy of the N–H bond is calculated for the ground and excited states by assuming adiabatic dissociation. An active space of 11 orbitals is used here to compare with the neutral radical states previously computed (Krauss and Garmer 1993).

For this case with transitions in the UV, it is not clear that a balanced improvement between the ground- and excited-state orbitals can be obtained by iterating ground-state natural orbitals. Energies were computed by iterating the natural orbitals for the ground state at both the X and T geometries, but in all cases the excited-state energies increased in energy. Convergent behavior is obtained with state-averaged natural orbitals, but such studies were not completed for indole. We also discovered that starting with vectors from an RHF calculation of the singlet ground state yields excited-state energies substantially higher than those started from ROHF vectors. In the first iterative natural orbital (INO) step using the ROHF vectors, the coupling between the ground and first excited state increases the energy of the excited state substantially and reduces the energy difference between the L_A and L_B states. Although this is in better agreement with the experiment, too much weight is apparently given to correlating the ground state relative to the first excited state. If orbitals are first determined by a singles only CI (CIS) starting with RHF vectors and then iterating on the FOCI natural orbitals with the active space including the one additional V orbital, this ultimately produces energies similar to those obtained with the ROHF vectors. Two levels of INO iteration were required, and these lowered the energies of ground and excited states. This latter procedure was chosen for the X geometry. The FOCI INO result starting with ROHF vectors
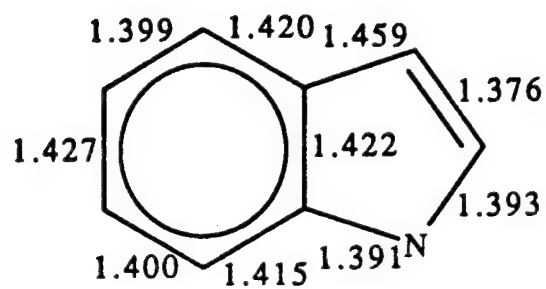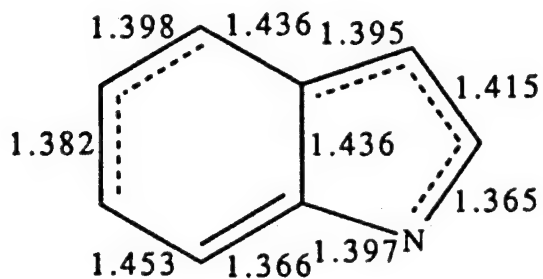
X Geometry (Ground HF)
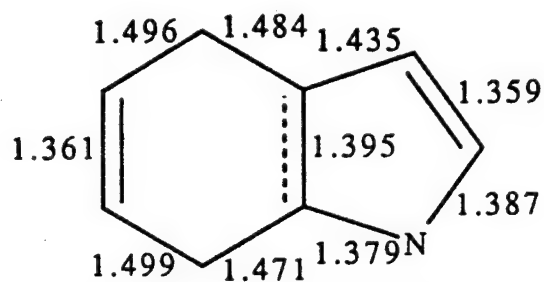
T Geometry and Schematic Bonding
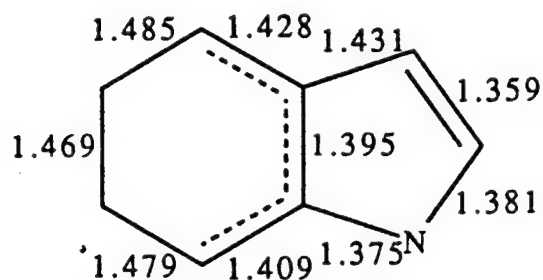
MC Geometry and Schematic Bonding

S1 Geometry and Schematic Bonding

Figure 1. Bond distances and schematic of π bonds: X geometry; T geometry; M geometry; and S1 geometry.

at the T geometry also led to a substantial increase in the energy of the L_B state. Since only the ground-state energy decreased in the INO procedure for the T geometry, the calculation used the initial ROHF vectors throughout for the T, M, and S1 geometries.

The dominant configurations and coefficients are presented for the four geometries in Table 2, illustrating the essential multiconfiguration character of the excited states. These coefficients also allow us to follow the excited states in the presence of the RF. Total energies, excitation energies, and dipole moments are given in Table 1, with the oscillator strengths and transition dipoles in Table 3. The in vacuo and RF results are compared in appropriate tables. Two iterations of the RF were done with the leveling off of the dipole moments suggesting an approach to convergence. The classical RF shifts are presented in Table 4.

3. DISCUSSION

The most important question concerns the relative ordering of the excited states in vacuo vs. in a solvent. From Table 1 we find that ΔE_{12} or $\Delta E_{A,B}$ is calculated to be 4,473 cm^{-1} at the X geometry in vacuo, which is substantially larger than the experimental value estimated from the FC maxima of about 2,800 cm^{-1} (Ilich, Haydock, and Prendergast 1989). Other estimates run as low as 1,100 cm^{-1} (Rizzo, Park, and Levy 1986) and as high as 3,700 cm^{-1} (Strickland, Horwitz, and Billups 1970). The absorption RF in water reduces the splitting by about 1,000 cm^{-1} to 3,424 cm^{-1}. The in vacuo energy separation is considerably smaller for the T (2,226 cm^{-1}) and S1 (2,372 cm^{-1}) geometries but remains large for the M geometry (4,554 cm^{-1}). The smaller energy separation between the L_B and L_A states at the T geometry arises entirely from the lower energy of the L_A state. This suggests that the T geometry is closer to the equilibrium geometry of the L_A state. At S1 both of the excited-state energies are above those for T and M. But we shall see further on in the discussion that the electronic structures of states 2 and 3 as seen through the transition dipole moments for S1 may not correspond, as they do at the other geometries, to states B and A, respectively.

RF calculations for absorption were not done at the T, M, and S1 geometries. However, since the static dipole moments for all states in the T and M geometries are similar to their corresponding states using the X geometry, we expect that the reduction in the separation between the L_A and L_B states would be about 1,000 cm^{-1} at these geometries. However, for S1 a smaller shift is expected since the dipole moments for all of its states are similar.

8

Table 2. Most Important Configurations (Coefficient 0.1) From In Vacuo FOCI Using Structure M (Orbitals 1–16 Constitute the V Space)

Ground State

CSF	Coefficient		Orbital Occupancies						
			12	13	14	15	16	22	
1	0.90	(2)	2	2	2	2	0	0	(0)
4	−0.10	(2)	2	1	2	2	1	0	(0)
5	0.25	(2)	1	2	2	2	1	0	(0)
7	−0.12	(2)	2	2	2	0	2	0	(0)
6107	−0.12	(2)	2	2	2	1	0	1	(0)

State 2 37,836 cm^{-1}

CSF	Coefficient		Orbital Occupancies								
			12	13	14	15	16	17	18	22	
2	−0.14	(2)	2	2	2	1	1	0	0	0	(0)
3	0.72	(2)	2	2	1	2	1	0	0	0	(0)
4	−0.32	(2)	2	1	2	2	1	0	0	0	(0)
6168	−0.18	(2)	2	2	1	1	1	0	0	1	(0)
6838	0.13	(2)	2	2	1	1	1	0	1	0	(0)
7447	−0.37	(2)	2	2	2	1	0	1	0	0	(0)
7454[a]	0.10	(2)	1	2	2	1	1	1	0	0	(0)
7508	−0.10	(2)	2	2	1	1	1	1	0	0	(0)
7509	0.14	(2)	2	1	2	1	1	1	0	0	(0)
7510[a]	−0.21	(2)	1	2	2	1	1	1	0	0	(0)

State 3 42,390 cm^{-1}

CSF	Coefficient		Orbital Occupancies						
			12	13	14	15	16	17	22	
2	0.65	(2)	2	2	2	1	1	0	0	(0)
3	0.32	(2)	2	2	1	2	1	0	0	(0)
4	0.44	(2)	2	1	2	2	1	0	0	(0)
5	0.26	(2)	1	2	2	2	1	0	0	(0)
10	0.17	(2)	1	2	2	1	2	0	0	(0)
6167	−0.12	(2)	2	2	2	0	1	0	1	(0)
6169	−0.11	(2)	2	1	2	1	1	0	1	(0)
7448	0.13	(2)	2	2	1	2	0	1	0	(0)

[a]Different spin couplings for configuration state functions (CSFs) 7454 and 7510.

9

Table 3. Indole Transition Probabilities and Oscillator Strengths

Geometry	Field	Transition Dipole (e-bohr)		Oscillator Strength	
		1,2	1,3	1,2	1,3
X	none	0.873	1.195	0.098	0.203
	X	0.842	1.187	0.091	0.197
	L_A	0.632	1.255	0.050	0.209
	exp absptn[a]			0.01–0.04	0.12
T	none	0.920	0.961	0.097	0.112
	L_A	0.851	1.029	0.075	0.121
M	none	0.834	0.879	0.080	0.100
	L_A	0.873	0.078	0.063	0.106
S1	none	0.999	1.476	0.128	0.205
	L_A	1.268	1.215	0.197	0.202

[a]Experimental data are summarized by Callis (1991).

Table 4. Classical Indole Red Shifts

Geometry	Absorption	Fluorescence
X[a]	−1,115	−2,537
M	−1,663	−3,194

Geometry	X, 1	L_A, 1
X[b]	−1,512	−2,955
M	−3,713	−5,915
exp	~−2,000	~−4,500

[a]In vacuo FOCI dipole moments are used.
[b]FOCI dipole moments are determined from RF constructed
for the initial state of the transition.

The transition moments from the ground state to the L_B and L_A excited states are the basis for the designations (Anderson et al. 1986) which are related to comparable transitions in perimeter π systems like naphthalene. For this correspondence to hold, the L_B state should have its transition dipole oriented along the long axis of the molecule. However, at the X geometry this is clearly not true, as seen in

Figure 2, in agreement with the semiempirical results (Anderson et al. 1986) and the experiments in crystals of indole derivatives (Yamamoto and Tanaka 1972; Albinsson and Norden 1992). Gasphase data have been analyzed to suggest a smaller angle (Mani and Lombardi 1969), but this result is more indirect. The present results also agree with experiment and the semiempirical results in finding the angle between the transition dipoles to the L_A and L_B states is closer to $90°$ or in the present case $66°$. At the M and T geometries, the first excited-state transition moment is oriented closer to the long axis of the molecule, but these geometries probably contribute only slightly to the ground-state absorption. The RF transition moments for M and T clearly show the reversal of the B and A states. The reported absorption transition moment (Callis 1991) for L_A is much larger than that for L_B, which is not in agreement with the calculated values which are closer in magnitude.

For the S1 geometry, the transition moments behave more like the RF values for M and T. Since this is also accompanied by a larger dipole moment for the first excited state, we suggest the first excited state more closely resembles the L_A state at the S1 geometry. However, the electronic structures of these states alter substantially as a function of geometry, and the correspondence of the moments does not necessarily describe a pseudocrossing of the states. This cannot be determined by calculations at only selected points as is done at this time.

Experimental ground-state dipole moments range from 0.814 to 0.936 e-bohr (1 e-bohr = 2.541765 Debye) (Glasser and Lami 1981; Sun and Song 1977), in good agreement with the theoretical predictions of 0.78–0.84. The excited-state values are only estimates deduced from RF theory models of the fluorescent shift or semiempirical calculations. There is general agreement among these models that the ground-state and L_B dipoles are comparable and the L_A dipole is at least 0.75 e-bohr larger as found for the ab initio dipoles. The dipole moments behave similarly for the X, M, and T geometries and are seen to be mostly oriented in the same direction. The RF dipole increases only modestly in absorption, with the ground-state value increasing from 0.8 to 1.1 e-bohr while the L_A dipole goes from 2.3 to 2.6 e-bohr.

The RF in water for fluorescence has a dramatic effect on the dipole moments and energies as seen in Figures 2 and 3. Since the L_A state has the largest dipole moment for the T and M geometries, the RF is large and expected to be most important. At the T geometry, the first iteration already inverts the L_B and L_A states with the L_A state now lower by 1,789 cm^{-1} and the inversion increasing to 2,847 cm^{-1} in the second iteration (see Table 1C). The dipole moment for the L_A state increases from 2.6 to 3.7 e-bohr and then to 4.1 e-bohr in the two iterations. The dipole moment suggests the iterations are converging.

11
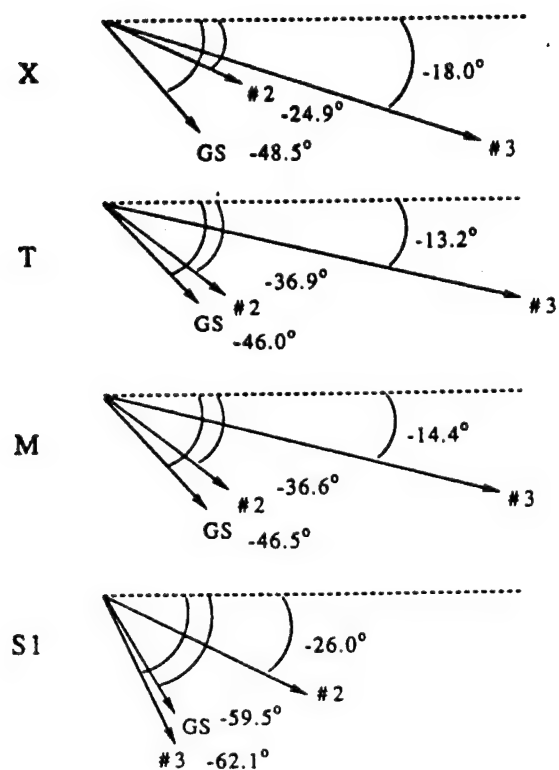
Figure 2. Transition dipole orientations relative to the indole long axis for excitation of both excited states from the ground state.
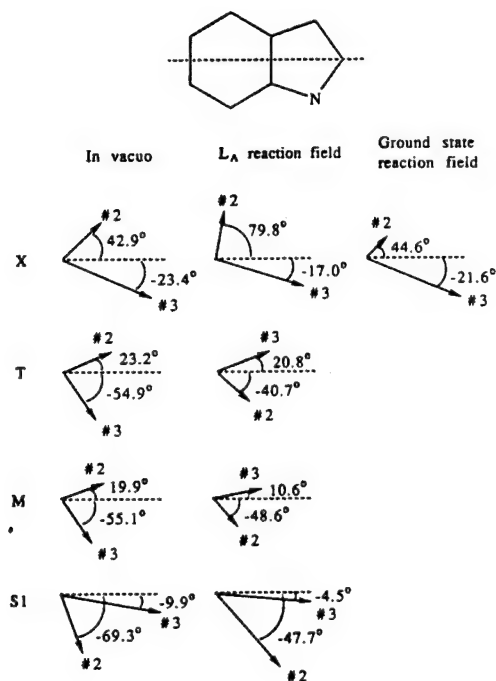
Figure 3. Dipole moment orientations relative to the indole long axis for all states.

At the M geometry, the first iteration yields a nearly degenerate set of states, but the A and B states are still unique electronically. The states invert in the next iteration as seen in Table 1. The RF dipole in L_A will be larger than 4.1 e-bohr. The L_B dipole moment is so similar to that of the ground state that there is only a small shift for fluorescence from the L_B state.

The L_A fluorescent RF interaction is weakest at the X geometry, where the first iteration only reduces the splitting to 2354 cm^{-1}. The dipole moment increases only to 2.7 e-bohr, and the states are still not inverted in the second iteration. At T and M geometries corresponding to the breaking of single π bonds, the excited states are more easily perturbed by the RF and very large dipole moments are produced. Only a few points on the surface have been explored, but it is evident that the excited-state energy minima are far from the X geometry. At these geometries the ground-state surface energy will have risen substantially, contributing to a large FC red shift. The energy surface of the L_B state is calculated to be relatively flat at the X and M points, which is consistent with the observation of a strong (0,0) band in absorption (Bersohn, Even, and Jortner 1984; Hager and Wallace 1984; Rizzo, Park, and Levy 1986; Strickland, Horwitz, and Billups 1970). The fluorescent solvent and FC shifts are described in a qualitative fashion in Figure 2.

Classical estimates of the shift in Table 4 used the FOCI dipole moments as was previously done for the radicals (Krauss and Garmer 1993). The classical and quantal values are similar, even though they differ in assumptions regarding the RF contributions from the permanent and polarization dipole of the solvent. Adiabatic dissociation energies for the N–H bond can be obtained since the radical energies are available (Krauss and Garmer 1993). The adiabatic asymptotes are presented schematically in Figure 4, and it is evident that only the ground state is bound with a dissociation energy of 317 kJ. No experimental value has been found for the dissociation of the N–H bond in indole. The L_B and L_A states are both calculated to be in the dissociative continuum by about 72 and 60 kJ, respectively. Significant questions need to be discussed regarding, first, the relative accuracy of the adiabatic limits and, second, the likelihood of barriers to dissociation in the energy surface. The indole excited states are calculated about 4000 cm^{-1} too high in energy with respect to the ground state, while the neutral radical excitation energies are much closer to experiment. This suggests that the relative energies of the excited states of indole and their respective neutral radical asymptotes can shift closer by up to 50 kJ.

The dissociation of the N–H bond should lead to a σ radical, but in vacuo both the ground and L_B states are connected adiabatically to π states, suggesting an energy surface barrier must be surmounted for

in vacuo   water

L_A ___   ___
___   ___   ___   σ   L_B ___
L_B ___   ___
                   ___   π   ___
                                  L_A

                   ___   π

       ___   Adiabatic   Solvent
X ___   FC shift asymptotes   shift
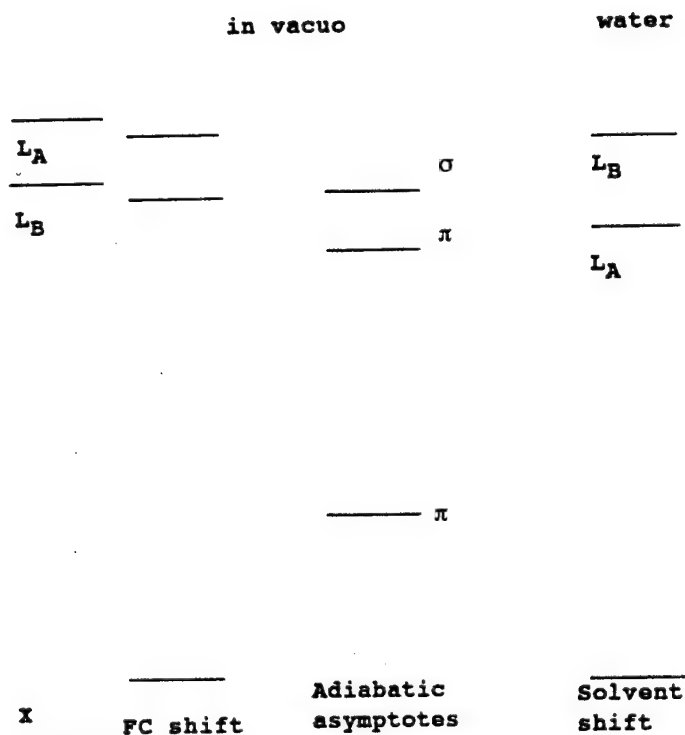
Figure 4.   Schematic of ground- and excited-state energies describing the FC shift and solvent shift.   Adiabatic dissociation limits of the N–H bond are given illustrating the dissociative character of both excited states, but only the L_A state connects with a σ radical and is likely to dissociate without a barrier.

dissociation.   However, the L_A state connects to a σ radical, and only a small barrier or no barrier is expected.   This supports the assertion that the lack of observation of the L_A state in nozzle experiments may be due as much to dissociation as to not exciting sufficiently high in energy (Glasser and Lami 1981). In water, the inversion of the populated excited states would alter the adiabatic behavior.   However, dissociation of the excited states should not be considered without explicit inclusion of first-shell hydrogen-bonded waters and other processes which can occur in solution.   Nothing conclusive can be determined on the dissociative properties of the excited states from this calculation because of the difficulty of accurate calculations, but the adiabatic analysis suggests that laser-induced fluorescence at the higher energies may search for emission from the radical excited states in the neighborhood of 580 nm (Krauss and Garmer 1993).

14

4. CONCLUSIONS

The large fluorescent red shift for indole in water is calculated to be due to two large and comparable contributions, FC and solvent shifts. Excitation into the M and T excited states breaks at least one of the π bonds on the benzene ring and distorts the equilibrium geometry from the ground state. This shift in equilibria is evident in the large FC envelope found in absorption especially for the L_A state (Anderson et al. 1986). With the RF present, the L_A state inverts with the L_B state and also will fluoresce to an excited part of the ground-state surface. The RF coupling to the L_A state is so large that it is likely that further distortion of the geometry will occur to maximize the dipole moment of the excited state. The present calculations find a very large dipole moment for the excited L_A state at the distorted geometries.

Lengthening the C_2–C_3 bond on the pyrrole ring apparently yields a first excited state with electronic characteristics closer to those of the L_A state. This state exhibits a substantial fluorescent red shift and always remains the first excited state. Excitation of bonds on the pyrrole ring apparently leads to a different electronic structure and ordering of states than excitations localized on the benzene ring, but the number of surface points studied here is too small to be more than suggestive.

The electronic properties of the excited states appear to be represented well by the FOCI calculation as gauged by the dipole moments and the orientation of the transition dipole moments at the X geometry. The relative energy difference between the L_A and L_B states is somewhat too large but qualitatively reasonable and decreases as the geometry distorts toward the excited-state equilibria. However, the excitation energies from the ground-state geometry are too large. The limitation in the number of active orbitals is certainly one cause that has to be examined in future studies. Ab initio calculations are shown to be needed to determine the variations in the moments and the response to reaction or environmental fields as a function of geometry. The FOCI appears to be sufficiently accurate for relative energies between the excited states, but the behavior as the active space of orbitals is expanded is required and awaits a more robust CI code than presently available.

INTENTIONALLY LEFT BLANK.

5. REFERENCES

Albinsson, B., and B. Norden. Journal of Physical Chemistry, vol. 96, p. 6204, 1992.

Anderson, B. E., R. D. Jones, A. A. Rehms, P. Ilich, and P. R. Callis. Chemical Physics Letters, vol. 125, p. 106, 1986.

Bender, C. F., and E. R. Davidson. Journal of Physical Chemistry, vol. 70, p. 2675, 1966.

Bersohn, R., U. Even, and J. Jortner. Journal of Chemical Physics, vol. 80, p. 1050, 1984.

Callis, R. R. Journal of Chemical Physics, vol. 95, p. 4230, 1991.

Creed, D. Photochem. Photobiol., vol. 39, p. 537, 1984.

Demmer, D. R., G. W. Leach, E. A. Outhouse, J. W. Hager, and S. C. Wallace. Journal of Physical Chemistry, vol. 94, p. 582, 1990.

Foresman, J. B., M. Head-Gordon, J. A. Pople, and M. J. Frisch. Journal of Physical Chemistry, vol. 96, p. 135, 1992.

Frisch, M. J., M. Head-Gordon, G. W. Trucks, J. B. Foresman, H. B. Schlegel, K. Raghavachari, M. A. Robb, J. S. Binkley, C. Gonzalez, D. J. Defrees, D. J. Fox, R. A. Whiteside, R. Seeger, C. F. Melius, J. Baker, R. L. Martin, L. R. Kahn, J. J. P. Stewart, S. Topiol, and J. A. Pople. Gaussian 90, Pittsburgh, PA: Gaussian, Inc., 1990.

Garmer, D. R. Presented at 1992 Sanibel Symposium.

Glasser, N., and H. Lami. Journal of Chemical Physics, vol. 74, p. 6526, 1981.

Hager, J. W., and S. C. Wallace. Journal of Physical Chemistry, vol. 88, p. 5513, 1984.

Hager, J. W., D. R. Demmer, and S. C. Wallace. Journal of Physical Chemistry, vol. 91, p. 1375, 1987.

Ilich, P., C. Haydock, and F. G. Pendergast. Chemical Physics Letters, vol. 158, p. 129, 1989.

Karle, I. I., K. Britts, and P. Gum. Acta Crystallogr., vol. 17, p. 496, 1964.

Karelson, M., and M. C. Zerner. Journal of American Chemistry Society, vol. 112, p. 9405, 1990.

Karelson, M., and M. C. Zerner. Journal of Physical Chemistry, vol. 96, p. 6949, 1992.

Krauss, M., and D. R. Garmer. Journal of Physical Chemistry, vol. 94, p. 831, 1993.

Krauss, M., and S. Roszak. Journal of Physical Chemistry, vol. 96, p. 8325, 1992.

Lami, H., and N. Glasser. Journal of Chemical Physics, vol. 84, p. 597, 1986.

Mani, A., and J. R. Lombardi. <u>J. Mol. Spectrose</u>, vol. 31, p. 308, 1969.

Rehms, A. A., and P. R. Callis. <u>Chemical Physics Letters</u>, vol. 140, p. 83, 1987.

Rizzo, T. R., Y. D. Park, and D. H. Levy. <u>Journal of Chemical Physics</u>, vol. 85, p. 6945, 1986.

Schmidt, M. W., J. A. Boatz, K. K. Baldridge, S. Koseki, M. S. Gordon, S. T. Elbert, and B. Lam. <u>GAMESS QCPE Bull.</u>, vol. 7, p. 115, 1987.

Stevens, W. J., H. Basch, and M. Krauss. <u>Journal of Chemical Physics</u>, vol. 81, p. 6026, 1984.

Strickland, E. H., J. Horwitz, and C. Billups. <u>Biochemistry</u>, vol. 9, p. 4914, 1970.

Sun, M., and P. S. Song. <u>Photochem. Photobiol.</u>, vol. 25, p. 3, 1977.

Suppan, P. <u>J. Photochem. Photobiol. A: Chem.</u>, vol. 50, p. 293, 1990.

Takigawa, T., T. Ashida, Y. Sasada, and M. Kakudo. <u>Bull. Chem. Soc. Jpn.</u>, vol. 39, p. 2369, 1966.

Tubergen, M. J., and D. H. Levy. <u>Journal of Physical Chemistry</u>, vol. 95, p. 2175, 1991.

Wong, M. W., M. J. Frisch, and K. B. Wiberg. <u>Journal of American Chemistry Society</u>, vol. 113, p. 4776, 1991.

Yamamoto, Y., and J. Tanaka. <u>Bull. Chem. Soc. Jpn.</u>, vol. 45, p. 1362, 1972.

NO. OF COPIES	ORGANIZATION
2	ADMINISTRATOR ATTN DTIC DDA DEFENSE TECHNICAL INFO CTR CAMERON STATION ALEXANDRIA VA 22304-6145
1	COMMANDER ATTN AMCAM US ARMY MATERIEL COMMAND 5001 EISENHOWER AVE ALEXANDRIA VA 22333-0001
1	DIRECTOR ATTN AMSRL OP SD TA US ARMY RESEARCH LAB 2800 POWDER MILL RD ADELPHI MD 20783-1145
3	DIRECTOR ATTN AMSRL OP SD TL US ARMY RESEARCH LAB 2800 POWDER MILL RD ADELPHI MD 20783-1145
1	DIRECTOR ATTN AMSRL OP SD TP US ARMY RESEARCH LAB 2800 POWDER MILL RD ADELPHI MD 20783-1145
2	COMMANDER ATTN SMCAR TDC US ARMY ARDEC PCTNY ARSNL NJ 07806-5000
1	DIRECTOR ATTN SMCAR CCB TL BENET LABORATORIES ARSENAL STREET WATERVLIET NY 12189-4050
1	DIR USA ADVANCED SYSTEMS ATTN AMSAT R NR MS 219 1 R&A OFC AMES RESEARCH CENTER MOFFETT FLD CA 94035-1000

NO. OF COPIES	ORGANIZATION
1	COMMANDER ATTN AMSMI RD CS R DOC US ARMY MISSILE COMMAND REDSTONE ARSNL AL 35898-5010
1	COMMANDER ATTN AMSTA JSK ARMOR ENG BR US ARMY TANK AUTOMOTIVE CMD WARREN MI 48397-5000
1	DIRECTOR ATTN ATRC WSR USA TRADOC ANALYSIS CMD WSMR NM 88002-5502
1	COMMANDANT ATTN ATSH CD SECURITY MGR US ARMY INFANTRY SCHOOL FT BENNING GA 31905-5660

ABERDEEN PROVING GROUND

NO. OF COPIES	ORGANIZATION
2	DIR USAMSAA ATTN AMXSY D AMXSY MP H COHEN
1	CDR USATECOM ATTN AMSTE TC
1	DIR USAERDEC ATTN SCBRD RT
1	CDR USACBDCOM ATTN AMSCB CII
1	DIR USARL ATTN AMSRL SL I
5	DIR USARL ATTN AMSRL OP AP L

20

24

NO. OF COPIES	ORGANIZATION	NO. OF COPIES	ORGANIZATION
1	VERITAY TECH INC ATTN E B FISHER 4845 MILLERSPORT HWY E AMHERST NY 14051-0305		ABERDEEN PROVING GROUND
1	FREEDMAN ASSOCIATES ATTN E FREEDMAN 2411 DIANA RD BALTIMORE MD 21209-1525	36	DIR USARL ATTN AMSRL WT P, A W HORST AMSRL-WT-PC, R A FIFER G F ADAMS W R ANDERSON R A BEYER S W BUNTE
6	ALLIANT TECHSYSTEMS ATTN J BODE C CANDLAND L OSGOOD R BURETTA R BECKER M SWENSON 600 SECOND ST NE HOPKINS MN 55343		C F CHABALOWSKI K P MCNEILL-BOONSTOPPEL A COHEN R CUMPTON R DANIEL D DEVYNCK N F FELL B E FORCH J M HEIMERL A J KOTLAR M R MANAA W F MCBRATNEY
1	US ARMY BENET LAB ATTN SAM SOPOK SMCAR CCB B WATERVLIET NY 12189		K L MCNESBY S V MEDLIN M S MILLER A W MIZIOLEK S H MODIANO J B MORRIS J E NEWBERRY S A NEWTON R PATEL R A PESCE RODRIGUEZ B M RICE R C SAUSA M A SCHROEDER J A VANDERHOFF M WENSING A WHREN J M WIDDER C WILLIAMSON

INTENTIONALLY LEFT BLANK.

USER EVALUATION SHEET/CHANGE OF ADDRESS

This Laboratory undertakes a continuing effort to improve the quality of the reports it publishes. Your comments/answers to the items/questions below will aid us in our efforts.

1. ARL Report Number _____ARL-TR-677_____ Date of Report _____February 1995_____

2. Date Report Received _____

3. Does this report satisfy a need? (Comment on purpose, related project, or other area of interest for which the report will be used.) _____

_____

_____

4. Specifically, how is the report being used? (Information source, design data, procedure, source of ideas, etc.) _____

_____

_____

5. Has the information in this report led to any quantitative savings as far as man-hours or dollars saved, operating costs avoided, or efficiencies achieved, etc? If so, please elaborate. _____

_____

_____

6. General Comments. What do you think should be changed to improve future reports? (Indicate changes to organization, technical content, format, etc.) _____

_____

_____

_____

_____
Organization

CURRENT
ADDRESS
_____
Name

_____
Street or P.O. Box No.

_____
City, State, Zip Code

7. If indicating a Change of Address or Address Correction, please provide the Current or Correct address above and the Old or Incorrect address below.

_____
Organization

OLD
ADDRESS
_____
Name

_____
Street or P.O. Box No.

_____
City, State, Zip Code

(Remove this sheet, fold as indicated, tape closed, and mail.)
(DO NOT STAPLE)